Brain Stimulation 18 (2025) 1871–1873

Contents lists available at ScienceDirect

Brain Stimulation

journal homepage: www.journals.elsevier.com/brain-stimulation

MRI-free targeting of deep brain regions using the 10–20 system

Dear Editor,

Many disorders of brain function involve neural networks situated deep in the brain, including limbic, basal ganglia, thalamic, and brain stem networks [1–3]. Emerging noninvasive neuromodulation techniques, including transcranial focused ultrasound [4] and spatially interfering electric fields [5] have the potential to modulate these deep brain structures selectively. However, these selective brain stimulation approaches require precise guidance, which has presented key challenges.

MRI-based neuronavigation [6] provides high accuracy, but the need to take MRI scans limits the accessibility and scalability of treatments. To address this, we have recently developed an MRI-free neuronavigation approach [7] based on fitting a template brain to anatomical landmarks of the head. Using facial anatomical landmarks, the approach can achieve 5.8 ± 3.0 mm (mean ± SD) accuracy for deep brain targets including the cingulate cortex and the anterior and posterior commissures. Although promising, this level of error is still large for selective targeting of deep brain nuclei and circuits [8].

To improve accuracy, in this study, we train and evaluate models that directly relate anatomical landmarks of the head, based on the standard 10–20 system, to specific brain targets. We find that this approach can target deep brain regions, acheiving sub-4 mm accuracy.

To train the models, we gathered T1-weighted scans of the head from 15 repositories available on OpenNeuro.org (RRID: SCR_005031). Identifiers can be found in the supplementary material. We included all subjects without severe defacing or known conditions associated with major structural abnormalities; 430 in total (mean ± SD age of 31.3 ± 11.0; nasion to inion distance of 357.1 ± 16.9 mm; LPA to RPA distance of 320.3 ± 19.4 mm; head circumference of 562.8 ± 20.9 mm; 53.2% female).

In these scans, we manually localized the principal anatomical landmarks of the 10–20 system: the nasion, left and right helix-scalp junctions (used instead of left and right preauricular points due to difficulty of localization in MRI), and the inion. The remaining 10–20 points were collected using a series of five image slices that connected principal markers, and percentile distances were measured along the resulting scalp perimeters. The 10–20 points included Fpz and Oz, thus providing 25 points in total. A detailed description of this process is available in the supplementary materials.

The brain regions were taken from the 696-parcel Yale Brain Atlas (YBA) [9], which spans 6 lobes, 38 sublobar brain regions, and 150 gyri. We used BrainSuite (RRID:SCR_006623, version 23a) to remove imaging artifacts and correct for nonuniformity. Subsequently, we used the linear and non-linear image registration tools in FSL (RRID:SCR_002823, version 6.0.7.16) to transform a template brain to each subject. Then, to find YBA regions in each patient, this transformation was applied to YBA coordinates derived from the same template.

We evaluated three models: a brain template registration model for comparison with the previous study [7], and two new model-based approaches. These approaches, based on linear models, map the 10–20 surface points to brain target coordinates. The first linear model used the Moore–Penrose pseudo-inverse. The second linear model used machine learning (ML) with an adaptive moment estimation optimizer and mean-squared error loss ($\eta = 0.001$, $\beta_1 = 0.9$, $\beta_2 = 0.99$). To evaluate generalizability, the models were trained and tested using leave-one-subject-out cross-validation, and results were averaged over all subjects. The prediction accuracy was measured as the Euclidean distance between the predicated and actual (YBA) target locations.

We evaluated the performance of the three models across all major brain regions (Fig. 1). The type of model had substantial leverage on the prediction accuracy (model main effect: $F_{2,1289} = 120$, $p < 0.001$, two-way repeated measures ANOVA), with the matrix inversion regression achieving the lowest error in all areas. As apparent from Fig. 1, the particular brain region also has significant leverage on the targeting accuracy (region main effect: $F_{18,23202} = 692.0$, $p < 0.001$, two-way repeated measures ANOVA). Moreover, there was a significant interaction between the two effects ($F_{36,23202} = 16.1$, $p < 0.001$).

We then analyzed cingulate and global targeting accuracy in depth and found that the matrix inversion model achieved the lowest mean error (Fig. 1, orange). For deep brain, cingulate targets (Fig. 1, Cingulate), the model attained an accuracy of 3.9 ± 1.7 mm (mean ± SD). For all brain regions defined in the YBA, the model attained an average 4.9 ± 2.5 mm accuracy (Fig. 1, Global Average). The accuracy of this model substantially exceeded our previous template matching approach [7], which produced errors of 5.2 ± 2.0 and 6.5 ± 2.8 mm, respectively (cingulate: $F_{2,838} = 80.9$, $p < 0.001$, one-way ANOVA; global average: $F_{2,821} = 129.1$, $p < 0.001$, one-way ANOVA). Games–Howell post-hoc analysis confirmed that both regression models outperformed template registration ($p < 0.001$), for both target groups.

This study evaluated the feasibility of predicting the coordinates of deep brain targets from 10–20 landmarks of the head, with the primary goal of eliminating the need for MRI. We found that the model-based approach used here provided substantially improved accuracy for targeting deep brain regions compared to our previous brain template registration approach [7]. Specifically, for deep brain targets, the previous method using facial anatomical landmarks achieved an

https://doi.org/10.1016/j.brs.2025.09.014
1 August 2025
Available online 1 October 2025

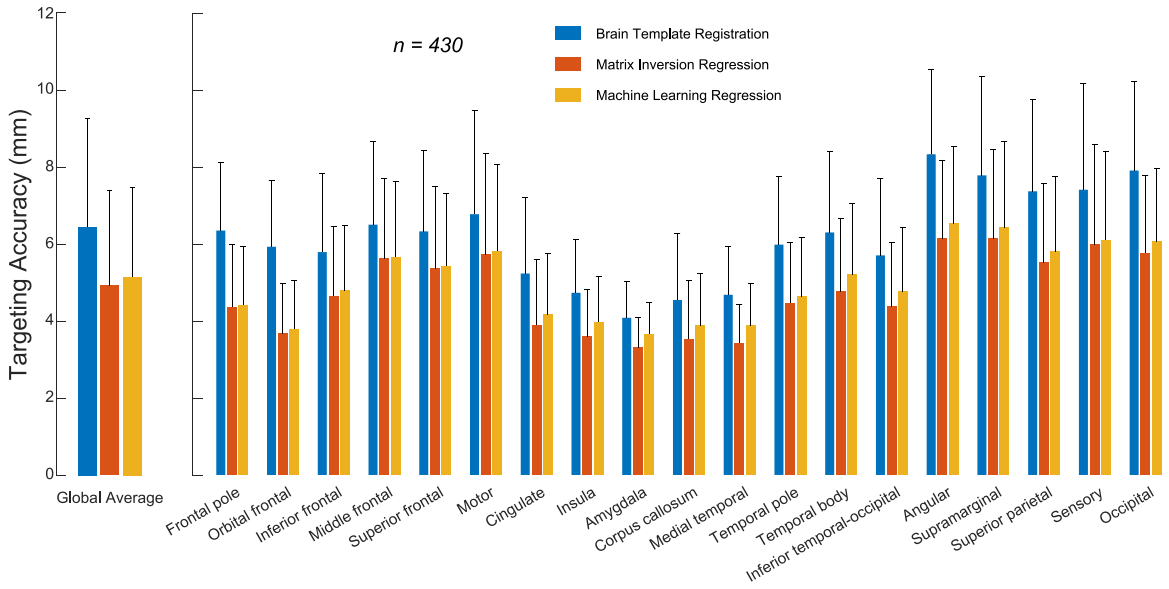

Fig. 1. Target prediction accuracy. Mean ± s.d. targeting accuracy, separately for each model (color), for the average across all regions (left), and for individual regions (right). Accuracy denotes the distance from true target. The models were trained and tested on data of 430 subjects using leave-one-subject-out cross-validation.

average accuracy of 5.8 mm [7], whereas the best-performing method in this paper (matrix inversion) achieved an accuracy of 3.9 mm—a 33% improvement.

These findings present a favorable tradeoff between targeting accuracy and the potential scaling of emerging brain stimulation approaches. Although higher accuracy could be achieved under MRI guidance, circumventing MRI increases access to treatments in areas where MRI is not available or its cost presents a substantial barrier.

Notably, the models in this study have been built on a training set in which the principal landmarks of the 10–20 system were labeled manually. Labeling these landmarks automatically would likely improve the consistency of the training set and thus improve the accuracy of the brain target prediction further. Additionally, because the landmarks in the training set were labeled using MRI, the results represent theoretical accuracy subject to error in clinical measurement of 10–20 markers. Our results (Suppl. Fig. 1) show that the machine learning regression is relatively insensitive to this error. Finally, this does not consider focal shifts due to subject-specific anatomy. Nonetheless, existing methods can address this issue. For instance, when using ultrasound, it is possible to account for these shifts without requiring a head MRI [10].

In summary, we provide a method for MRI-free targeting of deep brain structures based on standard 10–20 landmarks of the head. The model-based approaches are found to attain sub-4 mm accuracy, which can be sufficient for many emerging noninvasive brain stimulation approaches. Together, this study shows that it is possible to target deep brain structures based on easily accessible and routine measurements of 10–20 landmarks of the head, thus potentially circumventing the need for MRI.

CRediT authorship contribution statement

Tyler Nafziger: Writing – review & editing, Writing – original draft, Visualization, Software, Methodology, Investigation, Formal analysis, Data curation, Conceptualization. **Cecilia Phillips:** Writing – review & editing, Data curation. **Joshua Palter:** Writing – review & editing, Data curation. **Jan Kubanek:** Writing – review & editing, Supervision, Resources, Project administration, Funding acquisition, Conceptualization.

Declaration of competing interest

The authors declare the following financial interests/personal relationships which may be considered as potential competing interests: Jan Kubanek reports a relationship with SPIRE Therapeutics Inc. that includes: board membership and equity or stocks. All other authors declare that they have no known competing financial interests or personal relationships that could have appeared to influence the work reported in this paper.

Declaration of Generative AI and AI-assisted technologies in the writing process

During the preparation of this work the authors used ChatGPT 4o for text formatting. After using this tool, the authors reviewed and edited the content as needed and take full responsibility for the content of the published article.

Acknowledgments

This work was supported by grants from the National Institutes of Health (RF1NS128569) and NSF (CBET 2325125).

Supplementary data

Supplementary material related to this article can be found online at https://doi.org/10.1016/j.brs.2025.09.014.

References

[1] Johansen-Berg H, Gutman DA, Behrens TEJ, Matthews PM, Rushworth MFS, Katz E, Lozano AM, Mayberg HS. Anatomical connectivity of the subgenual cingulate region targeted with deep brain stimulation for treatment-resistant depression. Cerebral Cortex 2008;18(6):1374–83.

[2] Rodríguez-Cano E, Sarró S, Monté GC, Maristany T, Salvador R, McKenna PJ, Pomarol-Clotet E. Evidence for structural and functional abnormality in the subgenual anterior cingulate cortex in major depressive disorder. Psychol Med 2014;44(15):3263–73.

[3] Tye Kay M, Prakash Rohit, Kim Sung-Yon, Fenno Lief E, Grosenick Logan, Zarabi Hosniya, Thompson Kimberly R, Gradinaru Viviana, Ramakrishnan Charu, Deisseroth Karl. Amygdala circuitry mediating reversible and bidirectional control of anxiety. Nature 2011;471(7338):358–62.

[4] Tyler William J, Tufail Yusuf, Finsterwald Michael, Tauchmann Monica L, Olson Emily J, Majestic Cassondra. Remote excitation of neuronal circuits using low-intensity, low-frequency ultrasound. PLoS One 2008;3.
[5] Grossman Nir, Bono David, Dedic Nina, Kodandaramaiah Suhasa B, Rudenko Andrii, Suk Ho-Jun, Cassara Antonino M, Neufeld Esra, Kuster Niels, Tsai Li-Huei, et al. Noninvasive deep brain stimulation via temporally interfering electric fields. Cell 2017;169(6):1029–41.
[6] Rusjan Pablo M, Barr Mera S, Farzan Faranak, Arenovich Tamara, Maller Jerome J, Fitzgerald Paul B, Daskalakis Zafiris J. Optimal transcranial magnetic stimulation coil placement for targeting the dorsolateral prefrontal cortex using novel magnetic resonance image-guided neuronavigation. Hum Brain Mapp 2010;31:1643–52.
[7] Riis Thomas S, Lunt Seth, Kubanek Jan. MRI free targeting of deep brain structures based on facial landmarks. Brain Stimul 2025;18:131–7.
[8] Yamada K, Akazawa K, Yuen S, Goto M, Matsushima S, Takahata A, Nakagawa M, Mineura K, Nishimura T. MR imaging of ventral thalamic nuclei. Am J Neuroradiol 2010;31(4):732–5.
[9] McGrath Hari, Zaveri Hitten P, Collins Evan, Jafar Tamara, Chishti Omar, Obaid Sami, Ksendzovsky Alexander, Wu Kun, Papademetris Xenophon, Spencer Dennis D. High-resolution cortical parcellation based on conserved brain landmarks for localization of multimodal data to the nearest centimeter. Sci Rep 2022;12.
[10] Riis Thomas, Feldman Daniel, Mickey Brian, Kubanek Jan. Controlled noninvasive modulation of deep brain regions in humans. Commun Eng 2024;3.

Tyler Nafziger
Department of Biomedical Engineering, 36 S Wasatch Dr, Salt Lake City, UT 84112, United States of America

Cecilia Phillips
Department of Biomedical Engineering, 36 S Wasatch Dr, Salt Lake City, UT 84112, United States of America

Joshua Palter
Department of Electrical and Computer Engineering, 50 S Central Campus Dr #2110, Salt Lake City, UT 84112, United States of America

Jan Kubanek *
Department of Biomedical Engineering, 36 S Wasatch Dr, Salt Lake City, UT 84112, United States of America
E-mail address: jan.kubanek@utah.edu.

* Corresponding editor.